energies

MDPI

Article

# Analytical Approach to the Exergy Destruction and the Simple Expansion Work Potential in the Constant Internal Energy and Volume Combustion Process

**Jeongwoo Song and Han Ho Song ***

Department of Mechanical Engineering, Seoul National University, 1 Gwanak-ro, Gwanak-gu, Seoul 08826, Korea; nvergvup@snu.ac.kr

* Correspondence: hhsong@snu.ac.kr; Tel./Fax: +82-2-880-1651

Received: 7 December 2019; Accepted: 10 January 2020; Published: 13 January 2020




**Abstract:** The exergy destruction due to the irreversibility of the combustion process has been regarded as one of the key losses of an internal combustion engine. However, there has been little discussion on the direct relationship between the exergy destruction and the work output potential of an engine. In this study, an analytical approach is applied to discuss the relationship between the exergy destruction and efficiency by assuming a simple thermodynamic system simulating an internal combustion engine operation. In this simplified configuration, the exergy destruction during the combustion process is mainly affected by the temperature, which supports well-known facts in the literature. However, regardless of this exergy destruction, the work potential in this simple engine architecture is mainly affected by the pressure during the combustion process. In other words, if these pressure conditions are the same, increasing the system temperature to reduce the exergy destruction does not lead to an increase in the expansion work; rather, it only results in an increase in the remaining exergy after expansion. In a typical internal combustion engine, temperatures before combustion timing must be increased to reduce the exergy destruction, but increasing pressure before combustion timing is a key strategy to increase efficiency.

**Keywords:** combustion; exergy; exergy destruction; internal combustion engine; simple expansion work

## 1. Introduction

To satisfy either the strengthened fuel economy or carbon dioxide emission standards, many studies have been conducted to improve the internal combustion (IC) engine efficiency [1–3]. At the same time, studies are being conducted to analyze the inefficient factors in an IC engine. The analysis method of an IC engine can be divided into an energy analysis and an exergy analysis. The energy analysis is a method of analyzing how the lower heating value of the fuel is converted into work, heat, and exhaust energy [4,5]. However, the energy analysis has a drawback in that the quality difference between work and heat cannot be considered. To overcome these drawbacks, analysis using the exergy concept is being performed. Exergy is the maximum work that can be achieved by an interaction between the system and the environment [6]. Thus, the exergy can represent the quality difference between the work and heat. For example, even if the same amount of heat is transferred into the system, the increment of exergy is affected by the temperature of the system [7]. Therefore, some studies simultaneously perform the exergy analysis to discuss the available work in the IC engine operation, in addition to the energy analysis [7–10].

Exergy can be destroyed through an irreversible process, which means the available work of the system can decrease. There are several intrinsic irreversible processes in a spark-ignition (SI) engine,

such as fuel and air mixing, combustion [6,11,12], and heat transfer [13]. Many previous studies have shown that the exergy destruction of IC engines occurs mainly during the combustion process. Approximately 20% of the chemical exergy of fuel is destroyed during the combustion process [7,11,12], and studies have been conducted to suggest strategies to reduce the exergy destruction during the combustion process since this exergy destruction leads to a reduction in the system's available work [14,15]. These previous studies suggest increasing the temperature during the combustion process in order to reduce the exergy destruction by combustion. Increasing the temperature at which combustion occurs reduces the exergy destruction by the intermolecular heat transfer occurring at finite temperature differences during the combustion process [16]. However, strategies to reduce the exergy destruction do not necessarily lead to an increase in the IC engine efficiency [10,17,18]. This is because exergy represents the maximum work that can be obtained by a theoretical interaction between the system and environment; it does not consider the specific work extraction methods. In a real system, it is not always possible to turn a thermodynamic state of the system into an environment state through a reversible process.

In an IC engine, the sensible energy of the in-cylinder mixture is increased by the combustion process and then converted to the work through the expansion process. In this system, the maximum work that can be obtained is the pressure-volume work through the adiabatic expansion process [19,20]. Since the process to obtain the maximum work of the system is limited, the thermodynamic state of the mixture cannot be converted to the environmental thermodynamic state in a given architecture. This leads to the important points that it is not possible to convert all the thermomechanical exergy to a pressure-volume work and, therefore, there is no one-to-one relationship between the exergy destruction and the efficiency in an IC engine operation. As a result, a strategy for reducing the exergy destruction during the combustion process presented in previous studies may not necessarily lead to an efficiency increase. In addition, these studies did not explain how reducing the exergy destruction during the combustion process affects the efficiency.

This study aims to analyze the factors that reduce the exergy destruction and the factors that can increase the pressure-volume work in the simplified IC engine system. Then, the relationship between exergy destruction and pressure-volume work will be discussed in various initial thermodynamic state and compression ratio conditions. Especially, the analysis regarding asymmetric compression and expansion ratio is related to the Miller cycle or Atkinson cycle, which is applied in a modern IC engine, and will provide an explanation on its efficiency benefit and exergy destruction characteristic, as compared to those of the Otto cycle at the same compression ratio.

The main body of the paper is written in the following order. In Section 2, we introduce a simplified system to model and analyze the IC engine. Subsequently, in Section 3, the exergy destruction and pressure-volume work of the system are expressed analytically. Then, in Section 4, the effect of the initial thermodynamic states and compression ratio on exergy destruction and pressure-volume work is derived of an analytic form. Finally, in Section 5, the change in the exergy destruction and pressure-volume work according to the various work input method to the initial mixture are calculated through the simulation using a specific fuel.

## 2. System Description and Assumptions

### *2.1. System Description*

In this study, we considered a simple IC engine operation consisting only of the compression, combustion, and expansion processes without an additional compounding system in order to exploit either the remaining chemical exergy or the waste heat in the product gas. Therefore, there is only pressure-volume work available in this system. We simplified each process of the IC engine by applying an analytical approach to the system as follows. First, the initial reactant gas was compressed; then, the combustion process occurred under constant internal energy and volume at the top dead center. Finally, the burned gas was expanded to the mechanical equilibrium state with the environment to account

for the full potential of the pressure-volume work through expansion [21,22], although in a typical IC engine the gas expands by the expansion ratio as determined by the engine geometry. Figure 1 shows each process of the simplified system. The initial state of the system is state 1, the compressed state or the beginning of the combustion state is state 2, the end of combustion is state 3, and the state characterizing the expanded state of the gas after combustion into the mechanical equilibrium state where the environment is defined as state 3 m. Despite their simplicity, the suggested processes can capture most of the fundamental aspects of the IC engine operation by performing an exergy analysis.

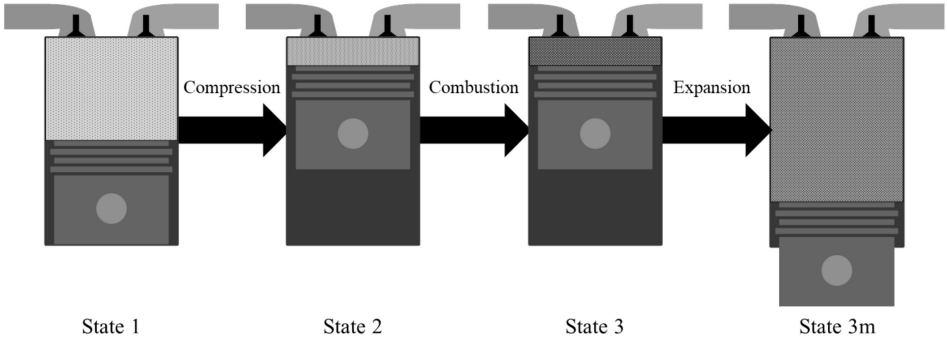



**Figure 1.** System configuration.

### 2.2. Major Assumptions

In this section, the major assumptions for each process and working fluid, which are made to derive the analytical expressions for the thermodynamic analysis of the system, were explained.

#### 2.2.1. Adiabatic System Assumption

In a typical IC engine operating condition, the system temperature is higher than the environment temperature. Therefore, if the heat transfer occurs, the system pressure-volume work is decreased. When all processes are assumed to be an adiabatic process, the maximum pressure-volume work from the system could be obtained.

#### 2.2.2. Constant Internal Energy and Volume Combustion Assumption

In a real IC engine, since the combustion process occurs over a finite time, the volume of the system changes during the combustion process. The change in volume during the combustion process can be similarly understood as there is a change in the initial condition and compression ratio for an infinitesimal mass burned. Thus, this study assumes that the combustion process occurs at a constant volume. Furthermore, this combustion process assumption can extract the maximum work in an IC engine [23–25].

#### 2.2.3. Uniformly Distributed Thermodynamic State

It is assumed that the state inside the system is uniform. This quasi-dimensional modeling method has been widely used for modeling IC engines [26–28]. If the thermodynamic states inside the system are uniform, then diffusion or convection does not occur inside the system. In addition, under constant internal energy and volume combustion assumption and an adiabatic assumption, the assumption of a uniform state does not affect the results because there is no interaction with the environment during each process.

In addition to the above assumptions, the working fluid is assumed to be an ideal gas mixture. The enthalpy, heat capacity, entropy, and chemical potential of the mixture are expressed using pure species values and Dalton's mixture rule. This assumption is a common assumption in engine modeling and does not strongly impact simulating real gases [29].

## 3. The Analytic Expression of Exergy Destruction and Simple Expansion Work

### *3.1. Exergy Destruction*

The exergy destruction during the combustion process can be calculated using the entropy generation of a chemical reaction.

$$X_{dest} = T_o \cdot s_{gen}, \tag{1}$$

The entropy generation can be obtained using the composition of the system and the chemical potential of the species under the constant internal energy and volume condition. From the $T\mathrm{d}S$ equation, the entropy changes in the uniform state system, which correspond to entropy generation under a given condition, can be written as Equation (2) [30]. In Equation (2), $T$ is the system temperature, $\mathrm{d}S$ is an infinitesimal entropy generation, $\mu_i$ is the chemical potential of species $i$, and $\mathrm{d}N_i$ is an infinitesimal mole number change of species $i$.

$$T\mathrm{d}S = -\sum_i \mu_i \mathrm{d}N_i, \tag{2}$$

The procedure for calculating the chemical potential of each species in Equation (2) is discussed below. First, using the Gibbs-Helmholtz equation, the chemical potential changes of each species are determined by the temperature change at constant pressure. In Equation (3), $h_i$ is the enthalpy of species $i$.

$$\frac{\partial}{\partial T}\left(\frac{N_i\mu_i}{T}\right)_p = -\frac{N_i h_i}{T^2}, \tag{3}$$

$$\frac{\mu_i(p_o, T)}{T} = \frac{\mu_i(p_o, T_o)}{T_o} + \int_{T_o}^{T} -\frac{h_i(p_o, T')}{T'^2}\mathrm{d}T', \tag{4}$$

The enthalpy of each species can be written as Equation (5). In Equation (5), $c_p$ is a specific heat at constant pressure of species $i$, and $h^f_{o,i}$ is an enthalpy of formation of species $i$.

$$h_i = h^f_{o,i} + \int_{T_o}^{T} c_{p,i}(T')\mathrm{d}T', \tag{5}$$

The chemical potential of each species at temperature $T$ and pressure $p$ can be expressed by using the chemical potential at temperature $T$ and pressure $p_o$ via the Gibbs-Duhem equation.

$$\mathrm{d}\mu_i = -s_i\mathrm{d}T + v_i\mathrm{d}p, \tag{6}$$

Here, $v_i$ is the specific volume of each species, and the assumptions in Section 2 are used, which can be written as follows:

$$v_i(p_i, T) = RT/p_i, \tag{7}$$

$$p_i = x_i \cdot p, \tag{8}$$

$$\mu_i(p, T) = \mu_i(p_o, T) + RT\ln(p_i/p_o), \tag{9}$$

Using Equations (4) and (9), the chemical potential at temperature $T$ and pressure $p$ can be expressed as the chemical potential at the reference state, the enthalpy of formation, the specific heat at constant pressure, and the partial pressure of each species. The chemical potential at the reference state is expressed as Equation (11). In Equation (11), $s_{o,i}$ is the entropy of species $i$ at reference state.

$$\frac{\mu_i(p, T)}{T} = \frac{\mu_i(p_o, T_o)}{T_o} + R\ln\frac{p_i}{p_o} + h^f_{o,i}\left(\frac{1}{T} - \frac{1}{T_o}\right) + \int_{T_o}^{T} -\frac{\int_{T_o}^{T'} c_p(T'')\mathrm{d}T''}{T'^2}\mathrm{d}T', \tag{10}$$

$$\mu_i(p_o, T_o) = h^f_{o,i} - T_o s_{o,i}, \tag{11}$$

Finally, in Equation (2), the entropy change of a single zone system during the combustion process can be expressed using Equations (10) and (11).

$$\mathrm{d}S = -\sum_i \left[ -s_{o,i} + \frac{h^f_{o,i}}{T} + R\ln x_i + R\ln\frac{p}{p_o} - \int_{T_o}^{T} \frac{\int_{T_o}^{T'} c_p(T'')\mathrm{d}T''}{T'^2}\mathrm{d}T' \right] \mathrm{d}N_i, \tag{12}$$

Entropy generation and exergy destruction can be obtained by integrating Equation (12) during the combustion process. Detailed integration procedure is shown in Appendix B. The entropy generation when 1 mole of reactant is burned during the combustion process is shown in Equation (13). In Equation (13), $s_{o,rxn}$ is the entropy difference between the reactant and the product at reference state, $\bar{c}_{p,r}$ is the average specific heat at constant pressure of the reactant, $\bar{c}_{p,p}$ is the specific heat at constant pressure of the reactant, and $N_{ratio}$ is the ratio of the mole numbers between the product and reactant.

$$s_{gen} = s_{o,rxn} - \left( \int_{T_o}^{T_2} \frac{\bar{c}_{p,r}(T)}{T}\mathrm{d}T - R\ln\frac{p_2}{p_o} \right) + N_{ratio}\left( \int_{T_o}^{T_3} \frac{\bar{c}_{p,p}(T)}{T}\mathrm{d}T - R\ln\frac{p_3}{p_o} \right), \tag{13}$$

The exergy destruction during the combustion process could be written as Equation (14).

$$X_{dest} = T_o \cdot s_{o,rxn} - T_o\left( \int_{T_o}^{T_2} \frac{\bar{c}_{p,r}(T)}{T}\mathrm{d}T - R\ln\frac{p_2}{p_o} \right) + N_{ratio} \cdot T_o\left( \int_{T_o}^{T_3} \frac{\bar{c}_{p,p}(T)}{T}\mathrm{d}T - R\ln\frac{p_3}{p_o} \right), \tag{14}$$

### 3.2. The System's Net Work

As shown in Figure 2, the net work of the system is given as the difference between Work 1 and Work 2. Work 2 is what can be achieved when expanding the gas in state 1 to the mechanical equilibrium state with the environment, which can be expressed as $X_{TM,1m} - X_{TM,1m}$. Work 1, the isentropic pressure-volume work, can be obtained by the work obtained through expansion minus the work required for compression, which can be expressed as $W_{expn} - W_{comp}$. Therefore, the system's net work is as follows:

$$W_{net} = W_{expn} - W_{comp} - N_{react}(X_{TM,1} - X_{TM,1m}), \tag{15}$$

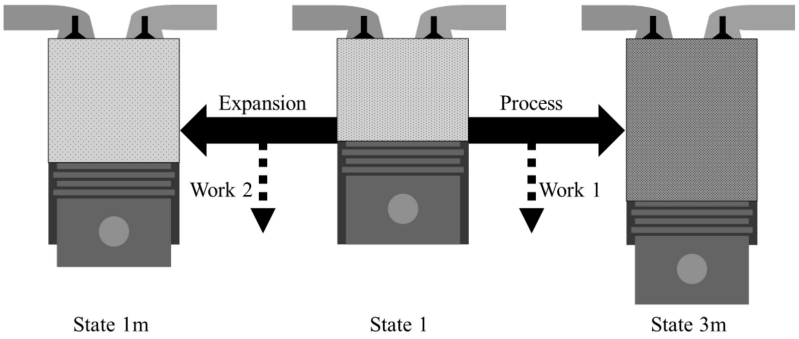



**Figure 2.** Pressure-volume work in the system from an initial state.

The difference between Work 2 and Work 1 is defined as the system's net work, which is an additional pressure-volume work that can be obtained by combustion. To understand the relationship between the exergy destruction and the pressure-volume work, this additional pressure-volume work is defined as the system's net work. $W_{expn}$ is the thermomechanical exergy difference between the before and after expansion. $W_{comp}$ can be calculated as the thermomechanical exergy difference before and after compression.

$$W_{expn} = N_{prod} \cdot (X_{TM,3} - X_{TM,3m}), \tag{16}$$

$$W_{comp} = N_{react} \cdot (X_{TM,2} - X_{TM,1}), \tag{17}$$

The system's net work per one mole of reactant is calculated as follows:

$$w_{net} = N_{ratio} \cdot (X_{TM,3} - X_{TM,3m}) - (X_{TM,2} - X_{TM,1m}), \tag{18}$$

Using the definition of thermomechanical exergy, a constant internal energy and volume combustion assumption, and an isentropic relation, Equation (18) can be rewritten as Equation (19).

$$w_{net} = -N_{ratio} h_{3m} + h_{1m}, \tag{19}$$

The system's net work can be written as Equation (20) using the heat of reaction, specific heat at constant pressure of reactant and product, and temperature at a mechanical dead state.

$$w_{net} = h_{o,rxn} - N_{ratio} \cdot \int_{T_o}^{T_{3m}} \bar{c}_{p,p}(T)dT + \int_{T_o}^{T_{1m}} \bar{c}_{p,r}(T)dT, \tag{20}$$

## 4. Exergy Destruction and System's Net Work Sensitivity

In Section 3, the exergy destruction by combustion and the system's net work are analytically expressed. The exergy destruction and system's net work derived in Section 3 are affected by the type of fuel, the constant pressure specific heat capacity of the mixture, and the temperature and pressure before and after combustion. This study aims to discuss the exergy destruction and pressure-volume work that typical IC engine operation. The results in Section 3 show that the temperature and pressure at before combustion timing affect exergy destruction and pressure-volume work for certain fuels. These thermodynamic conditions depend on the temperature and pressure of state 1 and the compression ratio. Therefore, in this section, we analyzed the effect of state 1 temperature, pressure, and compression ratio on exergy destruction and system's net work in an analytic method.

### *4.1. Initial Temperature*

In this section, the change in the exergy destruction and the system's net work caused by the combustion process when the temperature of the initial state changes is examined. The detailed derivation is described in Appendix C. The effects of the initial temperature on the exergy destruction and system's net work is shown in Equations (21) and (22), respectively.

$$\frac{\partial X_{dest}}{\partial T_1} = \frac{T_o}{T_1}\bar{c}_{v,r}(T_1)\left[\gamma_r(T_1)(N_{ratio} - 1) + \left(\frac{T_2}{T_3} - N_{ratio}\right)\right], \tag{21}$$

$$\frac{\partial w_{net}}{\partial T_1} = -\frac{\bar{c}_{v,r}(T_1)}{T_1}\left[T_{3m}\left((\gamma_r(T_1) - 1)N_{ratio} + \frac{T_2}{T_3}\right) - T_{1\mathrm{m}} \cdot \gamma_r(T_1)\right], \tag{22}$$

We have seen how the exergy destruction changes as the initial temperature changes. If the number of moles does not change before and after the combustion, Equation (21) can be written as follows:

$$\frac{\partial X_{dest}}{\partial T_1} = \frac{T_o}{T_1}\bar{c}_{v,r}(T_1)\left[\left(\frac{T_2}{T_3} - 1\right)\right], \tag{23}$$

In a typical IC engine, the temperature increases during the combustion process, so increasing the initial temperature reduces the exergy destruction. If the number of moles before and after the reaction changes, the exergy destruction decreases as the initial temperature increases in the reaction, which satisfies the Inequality (24).

$$N_{ratio} \leq \frac{\gamma_r(T_1) - T_2/T_3}{(\gamma_r(T_1) - 1)}, \tag{24}$$

Therefore, in reactions with a reduced number of moles, such as a hydrogen-air mixture, exergy destruction always decreases with increasing initial temperature. Even if the number of moles increases, the exergy destruction still decreases with increasing initial temperature if the condition in the Inequality (24) is satisfied. Figure 3 shows the above conditions according to $\gamma_r(T_1)$ and the temperature ratio before and after combustion. Here, if $N_{ratio}$ is greater than $N_{ratio,c}$ then initial temperature increases could rather lead to an increase in exergy destruction during the combustion process.

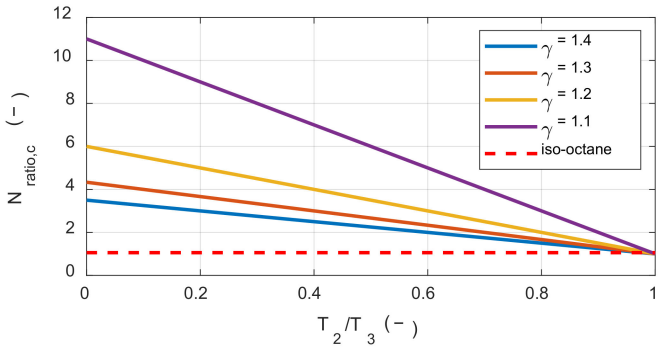



**Figure 3.** The critical molar ratio between the product and the reactant along with the temperature ratio and the specific heat ratio.

The stoichiometric mixture of iso-octane and air had a molar ratio of approximately 1.05 before and after the reaction. Therefore, when the temperature ratio before and after the reaction was approximately 0.98 or greater, the effect of the initial temperature on the exergy destruction was changed. However, it was not possible to achieve this temperature ratio by combustion of the stoichiometric mixture under typical IC engine operating conditions. This explains why the exergy destruction decreased under typical IC engine operating conditions with increased initial temperature.

Next, the effect of the initial temperature on the system's net work was investigated. Equation (22) is summarized as shown in Inequality (25). The detailed procedure is shown in Appendix C.

$$\frac{\partial w_{net}}{\partial T_1} \le -\bar{c}_{p,r}(T_1)\frac{T_{1m}}{T_1}\cdot f(p_r), where,\ f(p_r) = \left[\left(\frac{p_2}{p_o}\right)^{\frac{1}{\gamma_p(T_3)}-\frac{1}{\gamma_r(T_{1m})}}\left(\frac{p_2}{p_3}\right)^{-\frac{1}{\gamma_p(T_3)}}\left(1-\frac{1}{\gamma_r(T_1)}\left(1-\frac{p_2}{p_3}\right)\right)-1\right], \quad (25)$$

If the value inside the square bracket on the right side of Inequality (25) was positive, the system's net work decreased as the initial temperature increased. Therefore, in order to examine the condition in which the value of $f(p_r)$ is positive, the value of $f(p_r)$ was calculated along with the pressure ratio, as shown in Figure 4.

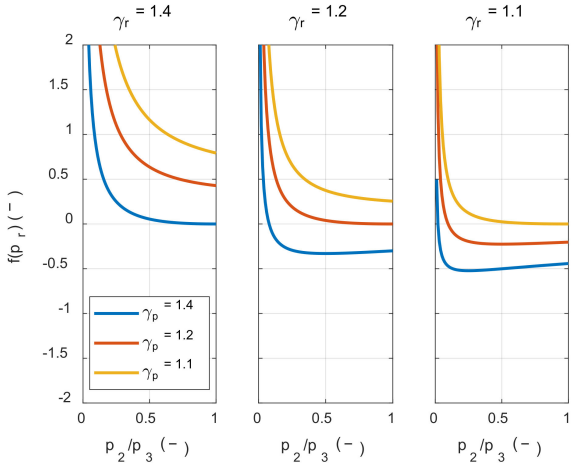



**Figure 4.** The effect of the pressure ratio and the specific heat ratio on the net work sensitivity of the initial temperature.

As shown in Figure 4, the value inside the square bracket was positive when the specific heat ratio of the product in state 3 was smaller than the reactant in state 1 m, regardless of the pressure ratio before and after combustion. In hydrocarbon fuels, which are mainly used in the IC engine, the specific heat ratio of the product was typically greater than that of the reactants at the same temperature. However, as the temperature increased, the specific heat ratio decreased by activating the vibrational energy mode of each molecule. Therefore, as shown in Figure 5, $\gamma_p(T_3)$ was smaller than $\gamma_r(T_{1m})$ when comparing the specific heat ratio of the product at the temperature after combustion and the specific heat ratio of the reactant at the temperature before combustion. As a result, the system's net work decreased as the initial temperature increased.

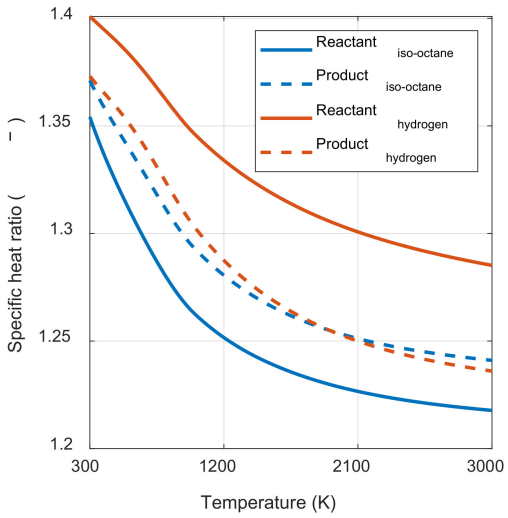



**Figure 5.** Specific heat ratio of iso-octane/air mixture and hydrogen/air mixture.

### *4.2. Initial Pressure*

By the ideal gas assumption, the specific heat capacity of the gas is not affected by the pressure. This assumption was used for calculating how the exergy destruction and system's net work are affected by the initial pressure. Detailed procedures are described in Appendix D.

$$\frac{\partial X_{dest}}{\partial p_1} = \frac{RT_o}{p_1}(1 - N_{ratio}), \tag{26}$$

$$\frac{\partial w_{net}}{\partial p_1} = \frac{R}{p_1}(N_{ratio}T_{3\mathrm{m}} - T_{1\mathrm{m}}), \tag{27}$$

If the number of moles before and after the combustion does not change, then the initial pressure does not affect the exergy destruction. If the number of moles before and after combustion is different, the exergy destruction is affected by the initial pressure and the ratio of the mole numbers between the product and reactant. This can be understood through Equation (A51). When the initial pressure is increased, the difference between the entropy change of reactant before combustion and the entropy change of product after combustion affects the entropy generation. When the initial pressure is increased, the decrease of entropy per reactant one mole and the decrease of entropy per product one mole are the same as shown in Appendix D. However, the entropy generation is affected by the initial pressure because the mole of product varies depending on the fuel when the one mole of reactant is burned. The exergy destruction was calculated when the initial pressures of iso-octane/air and hydrogen/air mixtures were increased under the complete combustion assumption, as shown in Figure 6. The iso-octane-air mixture with increasing molar numbers after combustion decreases the exergy destruction as the initial pressure increased, while the hydrogen-air mixture shows the opposite trend.

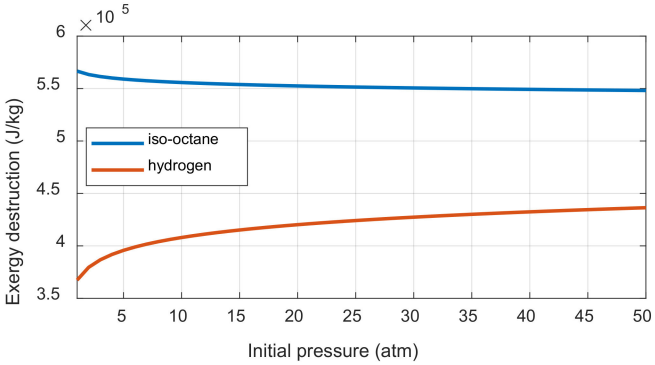



**Figure 6.** The exergy destruction changes of iso-octane and hydrogen combustion along with the initial pressure.

Next, we examined the effect of the initial pressure on system's net work. Equation (27) can be rewritten as shown in Inequality (28), with the detailed procedure described in Appendix D. In Inequality (28), state 3s means that the gas in state 3 expands until it has the same pressure as that in state 2.

$$\frac{\partial w_{net}}{\partial p_1} \geq \frac{RT_{1m}}{p_1}\left(\frac{V_{3s}}{V_3} - 1\right), \tag{28}$$

In a typical system, the pressure increases during the combustion process, so the system must expand to have the same pressure at the before combustion pressure. It means the volume at state 3s is larger than volume at state 3. Thus, the right side of Inequality (28) is greater than zero. Therefore, in a constant internal energy and volume combustion system, the system's net work increases as the initial pressure increases. Thus, the pressure-volume work that can be additionally obtained as the constant internal energy and volume combustion system increases through the combustion process.

### *4.3. Compression Ratio*

In the previous two cases, the effects of the mixture's initial thermodynamic state on the exergy destruction and the system's net work under a given geometrics condition were examined. In this section, we examined how the exergy destruction and system's net work caused by combustion change with the compression ratio when the initial mixture state is fixed. In the same thermodynamic state of the initial mixture, the effects of the elevated temperature and pressure before combustion due to the additional work during the compression process on the exergy destruction and the system's net work were examined. The detailed procedure was included in Appendix E.

$$\frac{\partial X_{dest}}{\partial CR} = \frac{RT_o}{CR} N_{ratio}\left[\frac{p_2}{p_3} - 1\right], \tag{29}$$

$$\frac{\partial \mathrm{w_{net}}}{\partial CR} = \frac{RT_{2m}}{CR} g(T_r), where,\ g(T_r) = \left[\frac{T_{3m}}{T_{2m}} \cdot \left(-\frac{T_2}{T_3} + N_{ratio}\right) + (N_{ratio} - 1)\gamma_r(T_2)\right], \tag{30}$$

Since the pressure at the end of combustion is higher than that at the start of combustion when a typical hydrocarbon is burned under constant internal energy and volume combustion conditions, the exergy destruction decreases as the compression ratio increases.

The effect of the compression ratio on the system's net work depends on the molar ratio before and after combustion. If the moles of the product are greater than or equal to the moles of the reactant, the system's net work always increases as the compression ratio increases, which is the case with typical hydrocarbon fuels. However, if the moles of the product are less than the moles of the reactant, the tendency now depends on the temperature ratio before and after combustion. To understand this latter effect, the sensitivity of the compression ratio in the hydrogen-air mixture was also examined. On the

right side of Equation (30), we investigated how the value of $g(T_r)$ was affected by the temperature before combustion as shown in Figure 7.

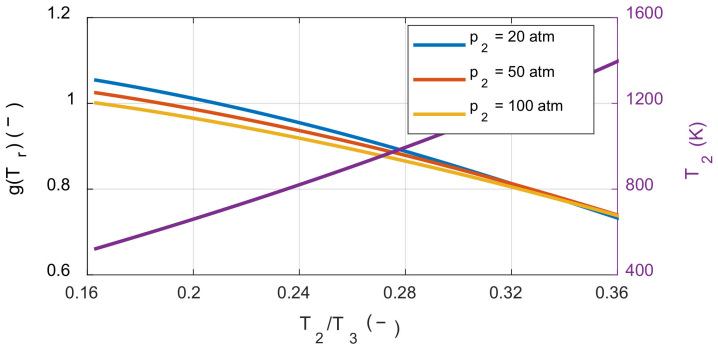



**Figure 7.** The effect of the temperature ratio and pressure before combustion on the net work sensitivity of the compression ratio.

When the values of $g(T_r)$ were calculated by varying the temperature and pressure before combustion, the values in the square bracket were greater than zero under all the calculated conditions. Therefore, even when using fuels for which molar number decreased after the combustion, such as hydrogen, the system's net work increased as the compression ratio increased under typical IC engine operating conditions. As a result, under typical IC engine operating conditions, increasing the compression ratio reduced the exergy destruction during the combustion process as well as increased the system's net work.

## 5. System Simulation

In Section 4, we analytically investigated the effect of the initial thermodynamic state and compression ratio on the exergy destruction and the system's net work. In this section, we examined how the exergy destruction and the system's net work changed when the thermodynamic state of the initial mixture changes, using the fuel-air mixture typically used for an IC engine modeling. When changing the thermodynamic state of the initial mixture with isobaric heating, isothermal compression, and isentropic compression, the exergy destruction, and the system's net work were examined along with the work input to change the thermodynamic state. It was assumed that the initial mixture is obtained by supplying the energy to the mixture at a thermomechanical dead state. The minimum work required to change the thermodynamics state of the initial mixture in three ways is the same as the thermomechanical exergy of state 1. The thermodynamic state and species composition of the environment required to calculate the exergy are shown in Table 1. The fuel used in this simulation was iso-octane, and the properties were taken from the information provided by Lawrence Livermore National Laboratory [31].

**Table 1.** Thermodynamic state and composition of the environment state.

| | |
|---|---|
| Pressure (atm) | 1 |
| Temperature (K) | 298.15 |
| $X_{CO_2}$ (−) | 0.00037 |
| $X_{H_2O}$ (−) | 0.03 |
| $X_{O_2}$ (−) | 0.7666 |
| $X_{N_2}$ (−) | 0.203 |

Figure 8 shows how the pressure and temperature of the initial mixture change with respect to the work input. Each marker indicated the work input at intervals of 0.01 for the chemical exergy of the initial mixture. Figure 8 shows how the thermodynamic state of the initial mixture changes through each process when the same work input is applied. If there is also another process that changes the

thermodynamic state of the initial mixture, it can be understood as the sum of the initial pressure change effect and the initial temperature change effect.

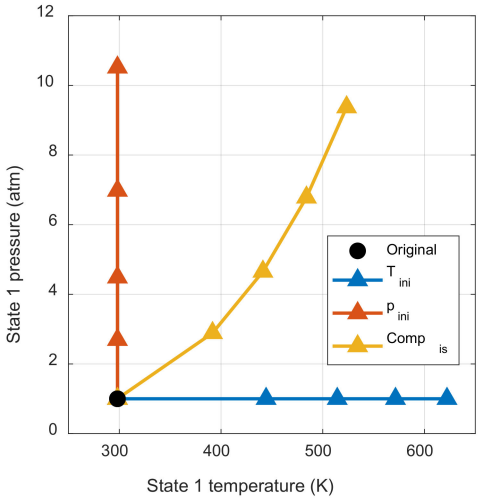



**Figure 8.** Initial thermodynamic state change by each process.

First, the effect of the initial mixture thermodynamic state change process on the exergy destruction during the combustion process was investigated. Figure 9 shows how the exergy destruction via combustion changes for the minimum energy required us to change the initial mixture's thermodynamic state. When the thermodynamic state of the initial mixture was altered in three ways, the isobaric heating process was the most effective way to reduce exergy destruction for the same work input. The next effective method was the adiabatic compression process and changing the state of the initial mixture with isothermal compression has little effect on the exergy destruction. Increasing the compression ratio reduced the exergy destruction during the combustion process for all initial mixture preparation methods. These results show that the temperature before combustion had a major effect on exergy destruction, as discussed in an analytical form in Section 4. Therefore, the exergy destruction during the combustion process was greatly reduced in the case of isobaric heating, adiabatic compression, and high compression ratio, which could increase the temperature before combustion.

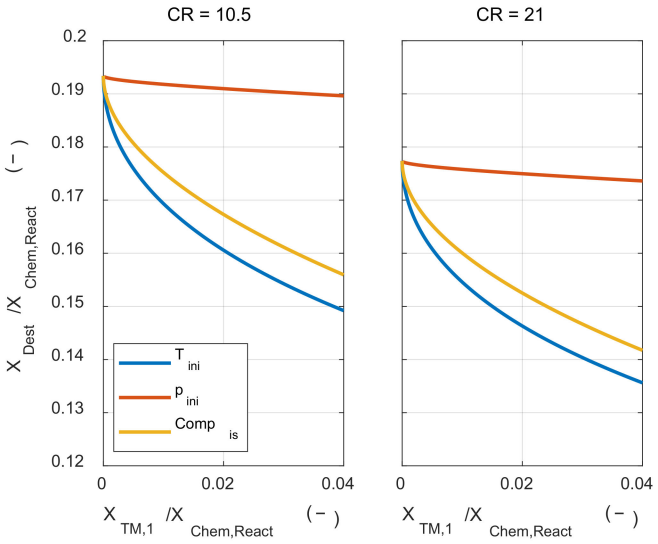



**Figure 9.** The exergy destruction under various initial thermodynamic states with a different compression ratio.

As described in many previous studies, this result shows that strategies to increase the reactant temperature would be effective in reducing the exergy destruction during the combustion process. When the exergy destruction was reduced, more of the chemical exergy of the fuel was converted to the thermomechanical exergy of the system. In the following paragraphs, we investigated whether this increased work potential could be cascaded down to the increased system's net work in the engine architecture. The pressure-volume work obtained when the system expanded to the initial volume like Acknowledgment IC engine, which is presented as a reference. In Figure 10, the solid line (—) shows that thermomechanical exergy was converted from chemical exergy by combustion, the dashed line (- -) shows the system's net work, and alternate long and short dashed line (– -) shows that work was obtained when the system expanded to the initial volume along with the work input of each process.

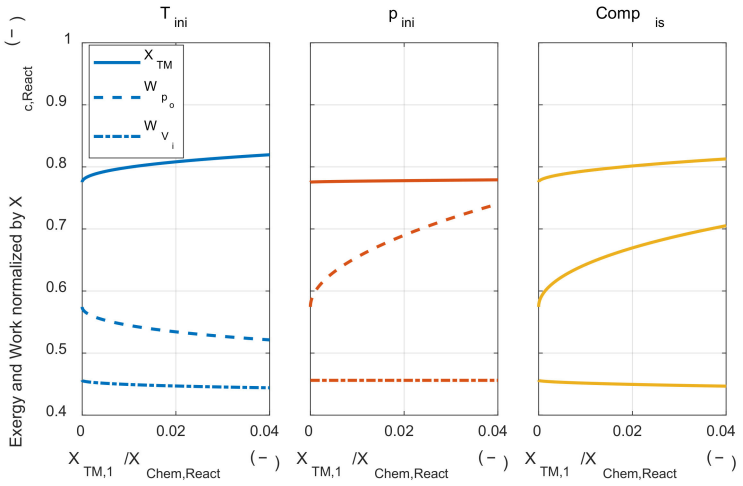



**Figure 10.** The exergy conversion, the system's net work, and work that is obtained by expanding to the initial volume under the various thermodynamic state changing process.

As the initial temperature increases, the converted thermomechanical exergy increased due to the lower exergy destruction during the combustion process, but the system's net work was decreased, and the work that could be obtained when expanded to the initial volume was hardly affected by the temperature change. This tendency can be explained using Equation (A40). In Equation (A40), when the change in $T_{3m}$ is larger than the change in $T_{1m}$ with respect to the change in initial temperature, the system's net work was reduced as increasing the initial temperature. In Section 4, the change in $T_{3m}$ and $T_{1m}$ was analytically obtained. The effect of the state 1 temperature change on state 3 m temperature could be qualitatively explained by the sum of the two effects. The first was that the state 3 temperature rose due to the state 1 temperature increase. The other was decreasing the expansion ratio when expanding to the environment pressure because the pressure decreased after the combustion. This is because the temperature ratio between the before combustion and the after combustion decreased as the temperature before combustion increases. Due to these two effects, the state 3 m temperature increase was greater than the state 1 m temperature increase when the state 1 temperature rose. Therefore, the system's net work was decreased as increasing the initial temperature. That is, even if the chemical exergy is more converted to thermomechanical exergy by increasing the initial temperature, it does not lead to the increase of work that can be obtained in a system that obtains pressure-volume work.

Next, the effect of isothermal compression on the system's net work was investigated. Higher initial pressure did not affect the conversion ratio from the chemical exergy to the thermomechanical exergy. However, the system' net work increased as the initial pressure increased. As the initial pressure increased, the work that could be obtained by expansion after combustion increased, but the work that could be obtained by expansion of the initial mixture also increased. As shown in Appendix D, the increase in the system's net work was proportional to the temperature difference

between the state 3 m and state 1 m. As mentioned in Section 4.2, the system's net work increased as the initial pressure increased in a typical IC engine because the temperature of state 3 m was higher than the temperature of state 1 m.

Finally, the effect of isentropic compression on the system's net work was investigated. Isentropic compression could be understood as the sum of the effects of initial temperature change and initial pressure change. The change in the thermodynamic state of the initial mixture with isentropic compression is shown in Figure 8. The system's net work increased because the pressure increase effect was greater than the temperature increase effect. Although the increase in the system's net work was lower than isothermal compression, both reduced exergy destruction and increased the system's net work could be achieved.

Next, the effect of the initial mixture thermodynamic state on the work that could be obtained when the system expands to the initial volume like a typical IC engine was investigated. All three methods of changing the initial mixture thermodynamic state did not significantly affect system work. Under the device expanding to the initial volume, the thermodynamic state of the initial mixture did not affect the pressure-volume work. It means that the work input was discharged from the system in the form of exhaust exergy.

With the change in the thermodynamic state of the initial mixture, how the compression ratio affects the pressure-volume work was investigated. In Figure 11, the exergy conversion ratio and the pressure-volume work was plotted when the compression ratio was increased from 10.5 to 21. In Figure 11, the gray-colored line was the result when the compression ratio was 10.5. When the compression ratio was increased, the tendency of the thermodynamic state of the initial mixture to pressure-volume work was not changed. However, when the compression ratio was increased, both the exergy conversion ratio and the pressure-volume work increased because the temperature and pressure before combustion timing were increased as the compression ratio was increased. Moreover, the pressure-volume work obtained when the system expanded to the initial volume was also increased. This pressure-volume work increase can be understood as the sum of two effects. The first is the increase of the pressure-volume work that can be obtained through the expansion due to increased pressure at before combustion timing due to the high compression ratio. The other is the increase of expansion ratio from the combustion timing to the end of expansion timing.

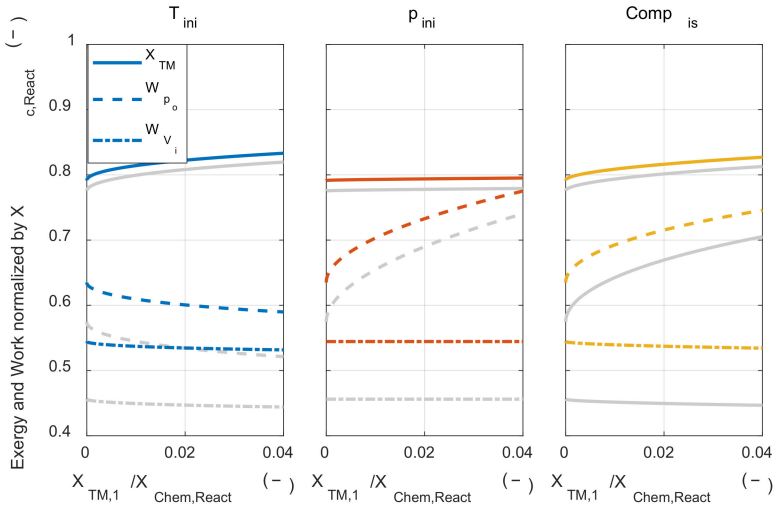



**Figure 11.** The exergy conversion, the system's net work, and work that is obtained by expanding to the initial volume under increased compression ratio.

## 6. Conclusions

This study aimed to improve the basic understanding of the relations between the exergy destruction during the combustion process and the efficiency in a system with a limited work extraction

method, such as an IC engine. The IC engine was simplified with the adiabatic process assumption, the constant internal energy and volume combustion assumption, and the uniform distribution of thermodynamic state assumption. Under the simplified system, the maximum work that could be obtained through the expansion and the exergy destruction during the combustion could be analytically expressed using the thermodynamic states, the heat of reaction, and the entropy change in reaction.

These analysis results indicated that the factors affecting the exergy destruction and the pressure-volume work were the thermodynamic state at the before combustion timing and the fuel. Therefore, for a specific fuel, the exergy destruction during the combustion process and the pressure-volume work could be calculated using the thermodynamic state at the before combustion timing, such as the temperature and the pressure. A sensitivity analysis was performed to understand how the thermodynamic state at the before combustion timing affects the exergy destruction and the pressure-volume work. As a result, increasing the temperature of the initial mixture or the compression ratio, which could increase the temperature at the before combustion timing, could reduce the exergy destruction during the combustion process. However, these strategies that increase the temperature before combustion timing reduced the pressure-volume work of system because the pressure-volume work was affected by the pressure before combustion timing and the pressure increase through the combustion process. Increasing the pressure of the initial mixture or the compression ratio, which increases the pressure at the before combustion timing, could increase the pressure-volume work. However, when the temperature of the initial mixture increased, it was confirmed that the pressure-volume work decreased due to the decrease in the pressure rise by combustion.

Then, the simulation results showed how the exergy destruction and the efficiency change with respect to the energy input required to change the thermodynamic states of the initial mixture under the iso-octane combustion situation. For the same work input, the exergy destruction decreased when the temperature at before combustion timing increased, and the pressure-volume work increased when the pressure at before combustion timing increased. However, the strategy that minimizes the exergy destruction reduced the pressure-volume work, and the strategy that maximizes the pressure-volume work hardly affected the exergy destruction. Moreover, even when the adiabatic assumption and complete combustion assumption were removed, those tendencies were maintained as shown in Appendix A.

A system, such as an IC engine, cannot convert all of the gas's thermomechanical exergy into the pressure-volume work. In a system with a limited work extraction method, in order to increase efficiency, the converted exergy must be in a suitable form for the system's work extraction method. The additional thermomechanical exergy that could be obtained by reducing the exergy destruction in an IC engine does not lead to efficiency improvement. Therefore, the strategies for reducing the exergy destruction discussed in many previous studies did not lead to efficiency improvement. Consequently, it is more important to discuss the strategies for increasing the efficiency, rather than minimizing the exergy destruction, in a system with limited work extraction methods.

**Author Contributions:** Conceptualization, J.S.; Methodology, J.S.; Software, J.S.; Supervision, H.H.S.; Writing—original draft, J.S.; Writing—review and editing, J.S. and H.H.S. All authors have read and agreed to the published version of the manuscript.

**Funding:** This work was supported by the Technology Innovation Program (No. 20002762, Development of RDE DB and Application Source Technology for Improvement of Real Road $CO_2$ and Particulate Matter) funded by the Ministry of Trade, Industry & Energy (MOTIE, Korea) through the Institute of Advanced Machinery and Design (IAMD) at Seoul National University.

**Conflicts of Interest:** The authors declare no conflict of interest.

## Nomenclature

| | |
|---|---|
| $c_p$ | Specific heat at constant pressure (J/kmol/K) |
| CR | Compression ratio |
| $c_v$ | Specific heat at constant volume (J/kmol/K) |
| H | Enthalpy (J/kmol) |
| N | Mole number (kmol) |
| $N_{ratio}$ | Ratio of the mole numbers between the product and reactant |
| P | pressure (Pa) |
| $p_o$ | Environment pressure (Pa) |
| R | Universal gas constant (J/kmol/K) |
| S | Entropy (J/K) |
| $s_{gen}$ | Entropy generation (J/kmol/K) |
| T | Temperature (K) |
| $T_o$ | Environment temperature (K) |
| V | specific volume ($m^3$/kmol) |
| $W_{net}$ | System's net work (J) |
| X | mole fraction |
| $X_{dest}$ | Exergy destruction (J/kmol) |
| $X_{TM}$ | Thermomechanical exergy (J/kmol) |
| Greeks | |
| Γ | Specific heat ratio |
| M | Chemical potential (J/kmol) |

## Appendix A Simulation Results When Two Major Assumptions Are Removed

The difference between the simplified system and real IC engine can occur by an adiabatic assumption and complete combustion assumption. The effect of those assumptions on the exergy destruction and system's net work was investigated through the simulation since it is difficult to investigate the influence of each assumption in an analytic method. The Hohenberg model [32,33] was adopted to model the heat transfer rate during the compression and expansion process, and the equilibrium state composition under the constant internal energy and volume condition was used to define the burned zone gas composition.

Firstly, the effect of those assumptions on the exergy destruction during the combustion process was examined. Figure A1 shows the results of three cases: when both assumptions were applied ('Adiabatic + Complete'), when only the adiabatic assumption was removed ('Complete only'), and when both assumptions were removed ('No assumption'). The tendency of the effect of initial temperature and pressure on the exergy destruction did not change without two major assumptions. However, when the adiabatic assumption was removed, the exergy destruction during the combustion process increased at the same initial temperature and pressure conditions, since the reduced temperature at the start of combustion timing due to the heat loss during the compression process.

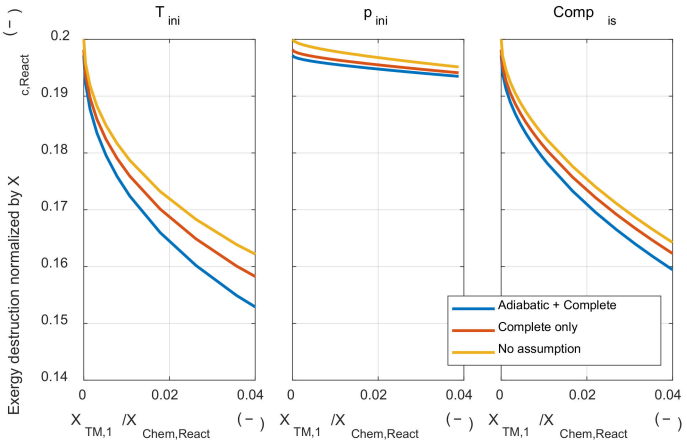



**Figure A1.** The exergy destruction under various initial thermodynamic states and relaxed major assumptions condition.

Next, the effect of those assumptions on the system's net work was examined. As shown in Figure A2, the two assumptions did not affect the tendency of the initial thermodynamic state to the system's net work.

When the adiabatic assumption was removed, the system's net work decreased, since the pressure during the expansion process decrease due to the heat transfer from the system to the environment. The system's net work was decreased when the complete combustion assumption was removed. This is because the rate of conversion from the chemical energy to the sensible energy through the combustion process was reduced when the complete combustion assumption was removed. The system's net work was decreased since the pressure rise through the combustion process was reduced.

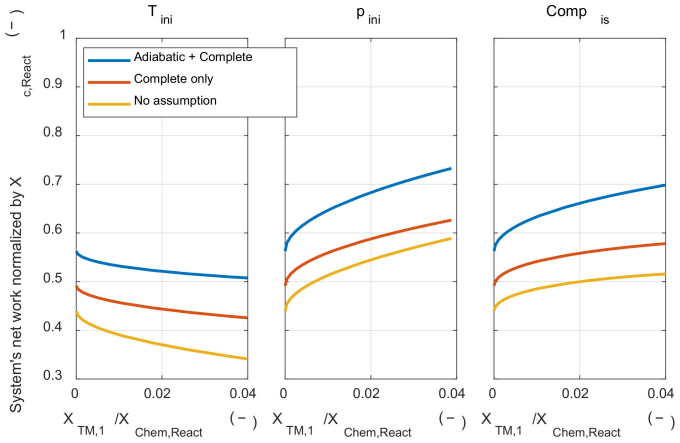



**Figure A2.** The system's net work under various initial thermodynamic states and relaxed major assumptions condition.

However, removing those two major assumptions did not affect the tendency of the effect of the initial temperature and pressure on the exergy destruction and system's net work. Therefore, the results discussed with the analytic method could be extended to the real IC engine operation.

## Appendix B Entropy Generation Derivation

The process of deriving Equation (13) from Equation (12) was described in detail in this section. Using the complete combustion assumption, it was assumed that only reactant and product exist inside the system during the combustion process. Therefore, the change in each species' number of moles in the system could be represented using the progress of reaction (ξ). Progress of reaction was assumed to be zero at the start of combustion and one at the end of combustion. The following relationship was used to derive Equation (13).

$$\ln x_{i,r}(\xi) = \ln\left(x_{i,r}(\xi = 0) \cdot \frac{1-\xi}{(1-\xi) + N_{ratio}\xi}\right), \tag{A1}$$

$$\ln x_{i,p}(\xi) = \ln\left(x_{i,p}(\xi = 1) \cdot \frac{N_{ratio}\xi}{(1-\xi) + N_{ratio}\xi}\right), \tag{A2}$$

$$\frac{\overline{h}^{f}_{o,r}}{T} - \int_{T_o}^{T} \frac{\int_{T_o}^{T'} \overline{c}_{p,r}(T'')\mathrm{d}T''}{T'^2}\mathrm{d}T' = -\int_{T_o}^{T} \frac{\overline{h}_r(T')}{T'^2}dT' + \frac{\overline{h}^{f}_{o,r}}{T_o}, \tag{A3}$$

Equation (A3) is rearranged as Equation (A4).

$$-\int_{T_o}^{T} \frac{\overline{h}_r(T')}{T'^2}dT' + \frac{\overline{h}^{f}_{o,r}}{T_o} = \frac{\overline{h}_r(T)}{T} - \int_{T_o}^{T} \frac{\overline{c}_{p,r}(T')}{T'}dT', \tag{A4}$$

In addition, the equation for the entropy change of ideal gas was used to simplify the equation.

$$\int_{T_o}^{T} \frac{\overline{c}_{p,r}(T')}{T'}dT' - R\ln\frac{p}{p_o} = \overline{s}_r(\xi) - \overline{s}_{o,r}, \tag{A5}$$

Therefore, Equation (12) can be expressed as the progress of reaction as follows:

$$\frac{dS}{N_o} = \left[R\ln\frac{1-\xi}{(1-\xi) + N_{ratio}\xi} + \frac{\overline{h}_r(T)}{T} - \overline{s}_r(\xi)\right]d\xi - \left[R\ln\frac{N_{ratio}\xi}{(1-\xi) + N_{ratio}\xi} + \frac{\overline{h}_p(T)}{T} - \overline{s}_p(\xi)\right]N_{ratio}d\xi, \tag{A6}$$

The first term inside the bracket can be summarized as Equation (A7).

$$\frac{dS_1}{N_o} = R[\ln(1-\xi) - N_{ratio}\ln(N_{ratio}\xi) - (1-N_{ratio})\cdot\ln(1+(N_{ratio}-1)\xi)]d\xi, \tag{A7}$$

Integrating for the progress of reaction is equivalent to Equation (A8).

$$\frac{S_1}{N_o} = R[-1 - N_{ratio}(\ln N_{ratio} - 1) + N_{ratio}\ln N_{ratio} - (N_{ratio}-1)] = 0, \tag{A8}$$

Therefore, Equation (A6) is summarized as follows:

$$\frac{dS}{N_o} = \left[\frac{\overline{h}_r(T) - N_{ratio}\overline{h}_p(T)}{T} - \overline{s}_r(\xi) + N_{ratio}\overline{s}_p(\xi)\right]d\xi, \tag{A9}$$

Equation (A9) can be re-written as Equation (A10) using the relationship between the enthalpy and internal energy.

$$\frac{dS}{N_o} = \left[\frac{\overline{u}_r(T) - N_{ratio}\overline{u}_p(T)}{T} + R(1-N_{ratio}) - \overline{s}_r(\xi) + N_{ratio}\overline{s}_p(\xi)\right]d\xi, \tag{A10}$$

Equation (A11) is made by the constant internal energy and volume combustion assumption.

$$\overline{u}_r(T_2) = N_{ratio}\overline{u}_p(T_3), \tag{A11}$$

Using Equation (A11), Equation (A10) can be written as follows:

$$\frac{dS}{N_o} = \left[\frac{\int_{T_2}^{T}\overline{c}_{v,r}(T')dT' + N_{ratio}\int_{T}^{T_3}\overline{c}_{v,p}(T')dT'}{T} - \overline{s}_r(\xi) + N_{ratio}\overline{s}_p(\xi) + R(1-N_{ratio})\right]d\xi, \tag{A12}$$

The internal energy balance inside the system during the combustion process can be expressed as follows:

$$\overline{u}_{o,r} + \int_{T_o}^{T_2}\overline{c}_{v,r}(T)dT = (1-\xi)\left(\overline{u}_{o,r} + \int_{T_o}^{T}\overline{c}_{v,r}(T\prime)dT\prime\right) + N_{ratio}\xi\left(\overline{u}_{o,p} + \int_{T_o}^{T}\overline{c}_{v,p}(T\prime)dT\prime\right), \tag{A13}$$

Differentiating Equation (A13) for the progress of reaction gives Equation (A14).

$$\left(\overline{u}_{o,r} + \int_{T_o}^{T}\overline{c}_{v,r}(T\prime)dT\prime\right) - N_{ratio}\left(\overline{u}_{o,p} + \int_{T_o}^{T}\overline{c}_{v,p}(T')dT'\right) = \left[(1-\xi)\overline{c}_{v,r}(T) + N_{ratio}\xi\overline{c}_{v,p}(T)\right]\frac{\partial T}{\partial\xi}, \tag{A14}$$

Substituting one for the progress of reaction in Equation (A13) gives the following equation.

$$\overline{u}_{o,r} - N_{ratio}\overline{u}_{o,p} = -\int_{T_o}^{T_2}\overline{c}_{v,r}(T)dT + N_{ratio}\int_{T_o}^{T_3}\overline{c}_{v,p}(T)dT, \tag{A15}$$

Equation (A16) can be obtained by substituting Equation (A15) into the Equation (A14).

$$\int_{T_2}^{T}\overline{c}_{v,r}(T')dT' + N_{ratio}\int_{T}^{T_3}\overline{c}_{v,p}(T')dT' = \left[(1-\xi)\overline{c}_{v,r}(T) + N_{ratio}\xi\overline{c}_{v,p}(T)\right]\frac{\partial T}{\partial\xi}, \tag{A16}$$

Then, the below equation can be obtained by substituting Equation (A16) into Equation (A12).

$$\frac{dS}{N_o} = \left[\frac{\left[(1-\xi)\overline{c}_{v,r}(T) + N_{ratio}\xi\overline{c}_{v,p}(T)\right]}{T}\frac{\partial T}{\partial\xi} - \overline{s}_r(\xi) + N_{ratio}\overline{s}_p(\xi) + R(1-N_{ratio})\right]d\xi, \tag{A17}$$

To summarize the above equation, the ideal gas equation was applied to the system during the combustion process.

$$p = \frac{p_2}{T_2}T\cdot(1-\xi+N_{ratio}\xi), \tag{A18}$$

Equation (A19) was obtained by differentiating the above equation with respect to the progress of reaction.

$$\frac{\partial p}{\partial \xi} = \frac{p_2}{T_2}(1 - \xi + N_{ratio}\xi)\frac{\partial T}{\partial \xi} + \frac{p_2}{T_2}T(N_{ratio} - 1), \tag{A19}$$

The above equation can be expressed as ($N_{ratio} - 1$) and substituted into Equation (A17) to obtain Equation (A20).

$$\frac{dS}{N_o} = \left[\frac{\left[(1-\xi)\bar{c}_{p,r}(T) + N_{ratio}\xi\bar{c}_{p,p}(T)\right]}{T}\frac{\partial T}{\partial \xi} - \frac{R}{p}(1 - \xi + N_{ratio}\xi)\frac{\partial p}{\partial \xi} - \bar{s}_r(\xi) + N_{ratio}\bar{s}_p(\xi)\right]d\xi, \tag{A20}$$

The above equation can be summarized as follows:

$$\frac{dS}{N_o} = \left[(1-\xi)\left(\frac{\bar{c}_{p,r}(T)}{T}\frac{\partial T}{\partial \xi} - \frac{R}{p}\frac{\partial p}{\partial \xi}\right) + N_{ratio}\xi\left(\frac{\bar{c}_{p,p}(T)}{T}\frac{\partial T}{\partial \xi} - \frac{R}{p}\frac{\partial p}{\partial \xi}\right) - \bar{s}_r(\xi) + N_{ratio}\bar{s}_p(\xi)\right]d\xi, \tag{A21}$$

In the above equation, the value inside the bracket is as follows:

$$\frac{\bar{c}_{p,r}(T)}{T}\frac{\partial T}{\partial \xi} - \frac{R}{p}\frac{\partial p}{\partial \xi} = \frac{d\bar{s}_r}{d\xi}, \tag{A22}$$

Substituting Equation (A22) into Equation (A21), Equation (A23) can be obtained.

$$\frac{dS}{N_o} = \left[(1-\xi)\left(\frac{d\bar{s}_r}{d\xi}\right) - \bar{s}_r(\xi) + N_{ratio}\xi\left(\frac{d\bar{s}_p}{d\xi}\right) + N_{ratio}\bar{s}_p(\xi)\right]d\xi, \tag{A23}$$

We can integrate the above equation with respect to the progress of reaction as follows:

$$\frac{S_{gen}}{N_o} = \left[(1-\xi)\cdot\bar{s}_r(\xi)\right]_0^1 + \left[N_{ratio}\xi\cdot\bar{s}_p(\xi)\right]_0^1, \tag{A24}$$

Therefore, the entropy generation from constant internal energy and volume combustion is as follows:

$$\frac{S_{gen}}{N_o} = -\bar{s}_r(T_2, p_2) + N_{ratio}\bar{s}_p(T_3, p_3), \tag{A25}$$

The entropy of reactant in state 2 and the entropy of product in state 3 can be represented by using the entropy of the reference state and the temperature and pressure of each state as follows:

$$\frac{S_{gen}}{N_o} = s_{o,rxn} - \left(\int_{T_o}^{T_2}\frac{\bar{c}_{p,r}(T)}{T}dT - R\ln\frac{p_2}{p_o}\right) + N_{ratio}\left(\int_{T_o}^{T_3}\frac{\bar{c}_{p,p}(T)}{T}dT - R\ln\frac{p_3}{p_o}\right), \tag{A26}$$

## Appendix C Initial Temperature Sensitivity

The effects of the initial temperature change on the exergy destruction and the system's net work were examined. First, Equation (14) was differentiated with respect to the initial temperature to investigate the effect on the exergy destruction.

$$\frac{\partial X_{dest}}{\partial T_1} = -T_o\left(\frac{\bar{c}_{p,r}(T_2)}{T_2}\frac{\partial T_2}{\partial T_1} - \frac{R}{p_2}\frac{\partial p_2}{\partial T_1}\right) + N_{ratio}T_o\left(\frac{\bar{c}_{p,p}(T_3)}{T_3}\frac{\partial T_3}{\partial T_1} - \frac{R}{p_3}\frac{\partial p_3}{\partial T_1}\right), \tag{A27}$$

To calculate Equation (A27), how the temperature and pressure of state 2 are affected by the initial temperature change needs to be known. These relations can be obtained using an isentropic relation and the ideal gas equation.

$$\frac{\bar{c}_{p,r}(T_2)}{T_2}\frac{\partial T_2}{\partial T_1} - \frac{\bar{c}_{p,r}(T_1)}{T_1} = \frac{R}{p_2}\frac{\partial p_2}{\partial T_1}, \tag{A28}$$

$$V_2\frac{\partial p_2}{\partial T_1} = R\left(T_2\frac{\partial N_1}{\partial T_1} + N_1\frac{\partial T_2}{\partial T_1}\right), \tag{A29}$$

The change in the mole number with respect to the temperature of state 1 was obtained using the ideal gas equation.

$$\frac{\partial N_1}{\partial T_1} = -\frac{N_1}{T_1}, \tag{A30}$$

Equations (A28)–(A30) can be summarized as follows:

$$\frac{\partial T_2}{\partial T_1} = \frac{\bar{c}_{v,r}(T_1)}{\bar{c}_{v,r}(T_2)} \cdot \frac{T_2}{T_1}, \tag{A31}$$

$$\frac{\partial p_2}{\partial T_1} = \frac{p_2}{T_1}\left(-1 + \frac{\bar{c}_{v,r}(T_1)}{\bar{c}_{v,r}(T_2)}\right), \tag{A32}$$

Next, the effects of state 1's temperature on state 3's temperature and pressure were calculated. These relations are obtained using a constant internal energy and volume combustion assumption.

$$u_{o,rxn} + \int_{T_o}^{T_2} \bar{c}_{v,r}(T)dT = N_{ratio} \int_{T_o}^{T_3} \bar{c}_{v,p}(T)dT, \tag{A33}$$

The effect of state 1's temperature on state 3's temperature can be expressed as follows using Equations (A29) and (A33).

$$\frac{\partial T_3}{\partial T_1} = \frac{1}{N_{ratio}} \frac{\bar{c}_{v,r}(T_1)}{\bar{c}_{v,p}(T_3)} \cdot \frac{T_2}{T_1}, \tag{A34}$$

Applying the ideal gas equation to state 3's gas, Equation (A35) can be obtained.

$$V_3 \frac{\partial p_3}{\partial T_1} = R\left(T_3 \frac{\partial N_3}{\partial T_1} + N_3 \frac{\partial T_3}{\partial T_1}\right), \tag{A35}$$

Equation (A35) can be summarized as Equation (A36) using Equations (A30) and (A34).

$$\frac{\partial p_3}{\partial T_1} = \frac{p_3}{T_3}\left(-\frac{T_3}{T_1} + \frac{1}{N_{ratio}} \frac{\bar{c}_{v,r}(T_1)}{\bar{c}_{v,p}(T_3)} \cdot \frac{T_2}{T_1}\right), \tag{A36}$$

To substitute the obtained relations into Equation (A27), the above relations are summarized as shown in Equations (A37) and (A38).

$$\frac{\bar{c}_{p,r}(T_2)}{T_2} \frac{\partial T_2}{\partial T_1} - \frac{R}{p_2} \frac{\partial p_2}{\partial T_1} = \frac{\bar{c}_{p,r}(T_1)}{T_1}, \tag{A37}$$

$$\frac{\bar{c}_{p,p}(T_3)}{T_3} \frac{\partial T_3}{\partial T_1} - \frac{R}{p_3} \frac{\partial p_3}{\partial T_1} = \frac{R}{T_1} + \frac{\bar{c}_{v,r}(T_1)}{N_{ratio}} \frac{T_2}{T_1 T_3}, \tag{A38}$$

Therefore, the effect of the initial temperature on the exergy destruction is as follows:

$$\frac{\partial X_{dest}}{\partial T_1} = \frac{T_o}{T_1} \bar{c}_{v,r}(T_1)\left(\gamma_r(T_1)(N_{ratio} - 1) + \left(\frac{T_2}{T_3} - N_{ratio}\right)\right), \tag{A39}$$

Next, the effect of the initial temperature on the system's net work was investigated.

$$\frac{\partial w_{net}}{\partial T_1} = -N_{ratio} \bar{c}_{p,p}(T_{3m}) \cdot \frac{\partial T_{3m}}{\partial T_1} + \bar{c}_{p,r}(T_{1m}) \cdot \frac{\partial T_{1m}}{\partial T_1}, \tag{A40}$$

The isentropic relation was used for calculating how the temperatures of states 3 m and 1 m are affected by the temperature of state 1.

$$\frac{\bar{c}_{p,p}(T_{3m})}{T_{3m}} \frac{\partial T_{3m}}{\partial T_1} - \frac{\bar{c}_{p,p}(T_3)}{T_3} \frac{\partial T_3}{\partial T_1} = -\frac{R}{p_3} \frac{\partial p_3}{\partial T_1}, \tag{A41}$$

Substituting Equations (A34) and (A36) into Equation (A41) can be summarized as follows:

$$\bar{c}_{p,p}(T_{3m}) \frac{\partial T_{3m}}{\partial T_1} = \frac{T_{3m}}{T_1}\left(R + \frac{\bar{c}_{v,r}(T_1)}{N_{ratio}} \cdot \frac{T_2}{T_3}\right), \tag{A42}$$

The effect on state 1 m's temperature is as follows:

$$\bar{c}_{p,r}(T_{1m})\frac{\partial T_{1m}}{\partial T_1} = \frac{T_{1m}}{T_1}\bar{c}_{p,r}(T_1), \tag{A43}$$

Substituting Equations (A42) and (A43) into Equation (A44) can be summarized as follows. This equation shows the effect of the temperature on the system's net work.

$$\frac{\partial w_{net}}{\partial T_1} = -N_{ratio}\frac{T_{3m}}{T_1}\left(R + \frac{\bar{c}_{v,r}(T_1)}{N_{ratio}}\cdot\frac{T_2}{T_3}\right) + \frac{T_{1m}}{T_1}\bar{c}_{p,r}(T_1), \tag{A44}$$

$$\frac{\partial w_{net}}{\partial T_1} = -\frac{\bar{c}_{v,r}(T_1)}{T_1}\left[T_{3m}\left((\gamma_r(T_1)-1)N_{ratio} + \frac{T_2}{T_3}\right) - T_{1m}\cdot\gamma_r(T_1)\right], \tag{A45}$$

Equation (A45) was summarized to investigate the effect of temperature on the system's net work.

$$\frac{\partial w_{net}}{\partial T_1} = -\bar{c}_{p,r}(T_1)\frac{T_{1m}}{T_1}\left[N_{ratio}\frac{T_{3m}}{T_{1m}}\left(\left(1 - \frac{1}{\gamma_r(T_1)}\right) + \frac{T_2}{T_3}\frac{1}{N_{ratio}}\frac{1}{\gamma_r(T_1)}\right) - 1\right], \tag{A46}$$

In Equation (A46), the following relation holds for $T_{3m}$ and $T_{1m}$.

$$T_{3m} \le T_3\left(\frac{p_3}{p_o}\right)^{-1+1/\gamma_p(T_3)}, \tag{A47}$$

$$T_{1m} \ge T_2\left(\frac{p_2}{p_o}\right)^{-1+1/\gamma_r(T_{1m})}, \tag{A48}$$

Equation (A46) can be summarized as Equation (A49) using the Equations (A47) and (A48).

$$\frac{\partial w_{net}}{\partial T_1} \le -\bar{c}_{p,r}(T_1)\frac{T_{1m}}{T_1}\left[\frac{p_3}{p_2}\left(\frac{p_3}{p_o}\right)^{-1+1/\gamma_p(T_3)}\left(\frac{p_2}{p_o}\right)^{1-1/\gamma_r(T_{1m})}\left(\left(1 - \frac{1}{\gamma_r(T_1)}\right) + \frac{p_2}{p_3}\frac{1}{\gamma_r(T_1)}\right) - 1\right], \tag{A49}$$

Summarizing Equation (A49) gives Equation (A50).

$$\frac{\partial w_{net}}{\partial T_1} \le -\bar{c}_{p,r}(T_1)\frac{T_{1m}}{T_1}\left[\left(\frac{p_2}{p_o}\right)^{\frac{1}{\gamma_p(T_3)}-\frac{1}{\gamma_r(T_{1m})}}\left(\frac{p_2}{p_3}\right)^{-\frac{1}{\gamma_p(T_3)}}\left(1 - \frac{1}{\gamma_r(T_1)}\left(1 - \frac{p_2}{p_3}\right)\right) - 1\right], \tag{A50}$$

## Appendix D Initial Pressure Sensitivity

Next, we investigated the effect of the initial pressure on the exergy destruction and the system's net work.

$$\frac{\partial X_{dest}}{\partial p_1} = -T_o\left(\frac{\bar{c}_{p,r}(T_2)}{T_2}\frac{\partial T_2}{\partial p_1} - \frac{R}{p_2}\frac{\partial p_2}{\partial p_1}\right) + N_{ratio}T_o\left(\frac{\bar{c}_{p,p}(T_3)}{T_3}\frac{\partial T_3}{\partial p_1} - \frac{R}{p_3}\frac{\partial p_3}{\partial p_1}\right), \tag{A51}$$

The isentropic relation and the ideal gas equation were used to calculate how state 2's temperature and pressure are affected by state 1's pressure.

$$\frac{\bar{c}_{p,r}(T_2)}{T_2}\frac{\partial T_2}{\partial p_1} = \frac{R}{p_2}\frac{\partial p_2}{\partial p_1} - \frac{R}{p_1}, \tag{A52}$$

$$V_2\frac{\partial p_2}{\partial p_1} = R\left(T_2\frac{\partial N_1}{\partial p_1} + N_1\frac{\partial T_2}{\partial p_1}\right), \tag{A53}$$

The above two equations are summarized as follows:

$$\frac{\bar{c}_{v,r}(T_2)}{T_2}\frac{\partial T_2}{\partial p_1} = 0, \tag{A54}$$

$$\frac{\partial p_2}{\partial p_1} = \frac{p_2}{p_1}, \tag{A55}$$

Next, we investigated how state 3's temperature and pressure are affected by state 1's pressure. Equation (A56) was obtained from the constant internal energy and volume combustion condition, and the ideal gas equation was used to calculate Equation (A57).

$$\bar{c}_{v,p}(T_3)\frac{\partial T_3}{\partial p_1} = \bar{c}_{v,r}(T_2)\frac{\partial T_2}{\partial p_1}, \tag{A56}$$

$$\frac{\partial p_3}{\partial p_1} = \frac{p_3}{p_1}, \tag{A57}$$

Based on the above relations, the effect of state 1's pressure on the exergy destruction is shown in Equation (A58).

$$\frac{\partial X_{dest}}{\partial p_1} = \frac{T_o R}{p_1}(1 - N_{ratio}), \tag{A58}$$

Next, the effect of state 1's pressure on the system's net work was investigated.

$$\frac{\partial w_{net}}{\partial p_1} = -N_{ratio}\bar{c}_{p,p}(T_{3m}) \cdot \frac{\partial T_{3m}}{\partial p_1} + \bar{c}_{p,r}(T_{1m}) \cdot \frac{\partial T_{1m}}{\partial p_1}, \tag{A59}$$

Equations (A60) and (A61) show how state 1's pressure affects the temperature of states 3 m and 1 m.

$$\frac{\bar{c}_{p,p}(T_{3m})}{T_{3m}} \cdot \frac{\partial T_{3m}}{\partial p_1} + \frac{\bar{c}_{p,p}(T_3)}{T_3} \cdot \frac{\partial T_3}{\partial p_1} = -\frac{R}{p_3} \cdot \frac{\partial p_3}{\partial p_1}, \tag{A60}$$

$$\frac{\bar{c}_{p,r}(T_{1m})}{T_{1m}} \cdot \frac{\partial T_{1m}}{\partial p_1} = -\frac{R}{p_1}, \tag{A61}$$

Substituting the above equations into Equation (A59) gives the equation below.

$$\frac{\partial w_{net}}{\partial p_1} = \frac{R}{p_1}(N_{ratio}T_{3\mathrm{m}} - T_{1\mathrm{m}}), \tag{A62}$$

To investigate how the system's net work changes as the initial pressure increases, the sign of the right side of Equation (A62) is examined.

$$\frac{\partial w_{net}}{\partial p_1} = \frac{RT_{1\mathrm{m}}}{p_1}\left(\frac{p_3}{p_2}\frac{T_2}{T_3}\frac{T_{3\mathrm{m}}}{T_{1\mathrm{m}}} - 1\right), \tag{A63}$$

$$\frac{\partial w_{net}}{\partial p_1} = \frac{RT_{1\mathrm{m}}}{p_1}\left(\frac{p_3}{p_2}\frac{T_{3s}}{T_3}\frac{T_2}{T_{3s}}\frac{T_{3\mathrm{m}}}{T_{2\mathrm{m}}} - 1\right), \tag{A64}$$

$T_{3s}$ is the temperature when the system expands from state 3 to state 2's pressure. Since the temperature of state 3s is higher than that of state 2, the following inequality holds for the typical hydrocarbon combustion process.

$$\frac{T_{3\mathrm{m}}}{T_{3s}} \geq \frac{T_{2\mathrm{m}}}{T_2}, \tag{A65}$$

Substituting Inequality (A65) into Equation (A64), the inequality below can be obtained.

$$\frac{\partial w_{net}}{\partial p_1} \geq \frac{RT_{1\mathrm{m}}}{p_1}\left(\frac{p_3}{p_2}\frac{T_{3s}}{T_3} - 1\right), \tag{A66}$$

Using the ideal gas state equation for state 3s and state 3, the inequality above is summarized as Inequality (A67).

$$\frac{\partial w_{net}}{\partial p_1} \geq \frac{RT_{1\mathrm{m}}}{p_1}\left(\frac{V_{3s}}{V_3} - 1\right), \tag{A67}$$

In general, since $V_{3s}$ is larger than $V_3$, the system's net work increases as the initial pressure increases.

## Appendix E Compression Ratio Sensitivity

The exergy destruction during the combustion process and the system's net work can be differentiated with respect to the compression ratio of the IC engine as follows. Changes in the compression ratio affect the

temperature and pressure after compression; thus, it can be understood as the sum of the effects of each parameter. The equation can be expressed as follows:

$$\frac{\partial \mathrm{f}}{\partial CR} = \frac{\partial f}{\partial T_2}\frac{\partial T_2}{\partial CR} + \frac{\partial f}{\partial p_2}\frac{\partial p_2}{\partial CR}, \tag{A68}$$

The equations below show the effect of the compression ratio on state 2's temperature and pressure using isentropic process relation.

$$\frac{\partial T_2}{\partial CR} = T_2 \cdot \frac{\gamma_r(T_2) - 1}{CR}, \tag{A69}$$

$$\frac{\partial p_2}{\partial CR} = p_2 \cdot \frac{\gamma_r(T_2)}{CR}, \tag{A70}$$

Substituting the above equations into Equation (A68), Equation (A71) was obtained.

$$\frac{\partial f}{\partial CR} = \frac{1}{CR}\left[(\gamma_r(T_2) - 1)T_2 \cdot \frac{\partial f}{\partial T_2} + \gamma_r(T_2)p_2 \cdot \frac{\partial f}{\partial p_2}\right], \tag{A71}$$

First, the effect of the compression ratio changing exergy destruction was analyzed. Equation (A72) was obtained by differentiating Equation (14) with respect to state 2's temperature

$$\frac{\partial X_{dest}}{\partial T_2} = -T_o\bar{c}_{v,r}(T_2)\left[\frac{\gamma_r(T_2)}{T_2} - \frac{\gamma_p(T_3)}{T_3} + \frac{\gamma_p(T_3) - 1}{T_3} - \frac{R}{T_3}\frac{p_3}{p_2}\frac{1}{\bar{c}_{v,r}(T_2)}\right], \tag{A72}$$

$$\frac{\partial X_{dest}}{\partial T_2} = -\bar{c}_{v,r}(T_2)\frac{T_o}{T_2}\left[\gamma_r(T_2)(N_{ratio} - 1) + \frac{T_2}{T_3} - N_{ratio}\right], \tag{A73}$$

Equation (A74) shows the effect of state 2's pressure changing exergy destruction.

$$\frac{\partial X_{dest}}{\partial p_2} = -R\frac{T_o}{p_2}[1 - N_{ratio}], \tag{A74}$$

Therefore, the sensitivity of the compression ratio on the exergy destruction can be calculated as follows:

$$\frac{\partial X_{dest}}{\partial CR} = \frac{RT_o}{CR}\left[\gamma_r(T_2)(N_{ratio} - 1) + \frac{T_2}{T_3} - N_{ratio} + \gamma_r(T_2)(1 - N_{ratio})\right], \tag{A75}$$

The above equation can be simplified as Equation (A76).

$$\frac{\partial X_{dest}}{\partial CR} = \frac{RT_o}{CR}\left[\frac{T_2}{T_3} - N_{ratio}\right], \tag{A76}$$

Next, we analyzed the effect of the compression ratio changing the system's net work. To confirm the sensitivity of the compression ratio on the system's net work, the partial derivative of the system's net work with respect to state 2's temperature and pressure were calculated. Equation (A78) shows the derivative with respect to state 2's temperature.

$$\frac{\partial \mathrm{w_{net}}}{\partial T_2} = -N_{ratio}\,\bar{\mathrm{c}}_{\mathrm{p,p}}(T_{3m}) \cdot \frac{\partial T_{3m}}{\partial T_2} + \bar{c}_{p,p}(T_{2m}) \cdot \frac{\partial T_{2m}}{\partial T_2}, \tag{A77}$$

$$\frac{\partial \mathrm{w_{net}}}{\partial T_2} = -N_{ratio}T_{3m}\left[\frac{c_p(T_3)}{T_3}\frac{\bar{c}_{v,r}(T_2)}{N_{ratio}\bar{c}_{v,p}(T_3)} - \frac{R}{T_2}\left(\frac{T_2}{T_3} \cdot \frac{\bar{c}_{v,r}(T_2)}{N_{ratio}\bar{c}_{v,p}(T_3)} - 1\right)\right] + \frac{T_{2m}}{T_2}c_p(T_2), \tag{A78}$$

Next, the derivative of the pressure of state 2 was calculated.

$$\frac{\partial w_{net}}{\partial p_2} = -N_{ratio}\bar{c}_{p,p}(T_{3m})\frac{\partial T_{3m}}{\partial p_2} + \bar{c}_{p,r}(T_{2M})\frac{\partial T_{2m}}{\partial p_2}, \tag{A79}$$

$$\frac{\partial w_{net}}{\partial p_2} = R\frac{T_{2m}}{p_2}\left(N_{ratio}\frac{T_{3m}}{T_{2m}} - 1\right), \tag{A80}$$

Therefore, the effect of the compression ratio changing the system's net work is as follows:

$$\frac{\partial w_{net}}{\partial CR} = \frac{RT_{2m}}{CR}\left[\frac{T_{3m}}{T_{2m}} \cdot \left(-\frac{T_2}{T_3} + N_{ratio}\right) + (N_{ratio} - 1)\gamma_r(T_2)\right], \quad \text{(A81)}$$

## References


1. Payri, F.; Luján, J.M.; Guardiola, C.; Pla, B. A challenging future for the IC engine: New technologies and the control role. *Oil Gas Sci. Technol. Rev. d'IFP Energies Nouv.* **2015**, *70*, 15–30. [CrossRef]
2. Yan, B.; Wang, H.; Zheng, Z.; Qin, Y.; Yao, M. The effect of combustion chamber geometry on in-cylinder flow and combustion process in a stoichiometric operation natural gas engine with EGR. *Appl. Therm. Eng.* **2018**, *129*, 199–211. [CrossRef]
3. Ravi, K.; Bhasker, J.P.; Alexander, J.; Porpatham, E. CFD study and experimental investigation of piston geometry induced in-cylinder charge motion on LPG fuelled lean burn spark ignition engine. *Fuel* **2018**, *213*, 1–11. [CrossRef]
4. Frigo, S.; Gentili, R. Analysis of the behaviour of a 4-stroke Si engine fuelled with ammonia and hydrogen. *Int. J. Hydrog. Energy* **2013**, *38*, 1607–1615. [CrossRef]
5. Fu, J.; Liu, J.; Wang, Y.; Deng, B.; Yang, Y.; Feng, R.; Yang, J. A comparative study on various turbocharging approaches based on IC engine exhaust gas energy recovery. *Appl. Energy* **2014**, *113*, 248–257. [CrossRef]
6. Verma, S.; Das, L.; Kaushik, S. Effects of varying composition of biogas on performance and emission characteristics of compression ignition engine using exergy analysis. *Energy Convers. Manag.* **2017**, *138*, 346–359. [CrossRef]
7. Caton, J.A. Exergy destruction during the combustion process as functions of operating and design parameters for a spark-ignition engine. *Int. J. Energy Res.* **2012**, *36*, 368–384. [CrossRef]
8. Amjad, A.; Saray, R.K.; Mahmoudi, S.; Rahimi, A. Availability analysis of n-heptane and natural gas blends combustion in HCCI engines. *Energy* **2011**, *36*, 6900–6909. [CrossRef]
9. Debnath, B.K.; Sahoo, N.; Saha, U.K. Thermodynamic analysis of a variable compression ratio diesel engine running with palm oil methyl ester. *Energy Convers. Manag.* **2013**, *65*, 147–154. [CrossRef]
10. Rakopoulos, C.D.; Giakoumis, E.G. Second-law analyses applied to internal combustion engines operation. *Prog. Energy Combust. Sci.* **2006**, *32*, 2–47. [CrossRef]
11. Dhyani, V.; Subramanian, K. Experimental based comparative exergy analysis of a multi-cylinder spark ignition engine fuelled with different gaseous (CNG, HCNG, and hydrogen) fuels. *Int. J. Hydrog. Energy* **2019**, *44*, 20440–20451. [CrossRef]
12. Chavannavar, P.; Caton, J. Destruction of availability (exergy) due to combustion processes: a parametric study. *Proc. Inst. Mech. Eng. Part A J. Power Energy* **2006**, *220*, 655–668. [CrossRef]
13. Bejan, A. Second-law analysis in heat transfer and thermal design. In *Advances in Heat Transfer*; Elsevier: Amsterdam, The Netherlands, 1982; pp. 1–58.
14. Daw, C.S.; Chakravarthy, V.K.; Conklin, J.C.; Graves, R.L. Minimizing destruction of thermodynamic availability in hydrogen combustion. *Int. J. Hydrog. Energy* **2006**, *31*, 728–736. [CrossRef]
15. Chakravarthy, V.K.; Daw, C.S.; Pihl, J.A.; Conklin, J.C. Study of the theoretical potential of thermochemical exhaust heat recuperation for internal combustion engines. *Energy Fuels* **2010**, *24*, 1529–1537. [CrossRef]
16. Dunbar, W.R.; Lior, N. Sources of combustion irreversibility. *Combust. Sci. Technol.* **1994**, *103*, 41–61. [CrossRef]
17. Caton, J.A. The thermodynamic characteristics of high efficiency, internal-combustion engines. *Energy Convers. Manag.* **2012**, *58*, 84–93. [CrossRef]
18. Sezer, İ.; Bilgin, A. Effects of charge properties on exergy balance in spark ignition engines. *Fuel* **2013**, *112*, 523–530. [CrossRef]
19. Liu, H.; Ma, J.; Tong, L.; Ma, G.; Zheng, Z.; Yao, M. Investigation on the potential of high efficiency for internal combustion engines. *Energies* **2018**, *11*, 513.
20. Taymaz, I.; Çakır, K.; Mimaroglu, A. Experimental study of effective efficiency in a ceramic coated diesel engine. *Surf. Coat. Technol.* **2005**, *200*, 1182–1185. [CrossRef]
21. Li, T.; Zheng, B.; Yin, T. Fuel conversion efficiency improvements in a highly boosted spark-ignition engine with ultra-expansion cycle. *Energy Convers. Manag.* **2015**, *103*, 448–458. [CrossRef]

22. Zhao, J. Research and application of over-expansion cycle (Atkinson and Miller) engines–A review. *Appl. Energy* **2017**, *185*, 300–319. [CrossRef]
23. Akansu, S.O.; Dulger, Z.; Kahraman, N.; Veziroğlu, T.N. Internal combustion engines fueled by natural gas—hydrogen mixtures. *Int. J. Hydrog. Energy* **2004**, *29*, 1527–1539. [CrossRef]
24. Hiyoshi, R.; Aoyama, S.; Takemura, S.; Ushijima, K.; Sugiyama, T. *A Study of a Multiple-Link Variable Compression Ratio System for Improving Engine Performance*; 2006-01-0616; SAE Technical Paper: Warrendale, PA, USA, 2006.
25. Ikeya, K.; Takazawa, M.; Yamada, T.; Park, S.; Tagishi, R. Thermal efficiency enhancement of a gasoline engine. *SAE Int. J. Engines* **2015**, *8*, 1579–1586. [CrossRef]
26. Fiveland, S.B.; Assanis, D.N. Development and validation of a quasi-dimensional model for HCCI engine performance and emissions studies under turbocharged conditions. *SAE Trans.* **2002**, *111*, 842–860. [CrossRef]
27. Verhelst, S.; Sierens, R. A quasi-dimensional model for the power cycle of a hydrogen-fuelled ICE. *Int. J. Hydrog. Energy* **2007**, *32*, 3545–3554. [CrossRef]
28. Qi, K.; Feng, L.; Leng, X.; Du, B.; Long, W. Simulation of quasi-dimensional combustion model for predicting diesel engine performance. *Appl. Math. Model.* **2011**, *35*, 930–940. [CrossRef]
29. Depcik, C.; Jacobs, T.; Hagena, J.; Assanis, D. Instructional use of a single-zone, premixed charge, spark-ignition engine heat release simulation. *Int. J. Mech. Eng. Educ.* **2007**, *35*, 1–31. [CrossRef]
30. Nishida, K.; Takagi, T.; Kinoshita, S. Analysis of entropy generation and exergy loss during combustion. *Proc. Combust. Inst.* **2002**, *29*, 869–874. [CrossRef]
31. Curran, H.J.; Gaffuri, P.; Pitz, W.J.; Westbrook, C.K. A comprehensive modeling study of iso-octane oxidation. *Combust. Flame* **2002**, *129*, 253–280. [CrossRef]
32. Sanli, A.; Sayin, C.; Gumus, M.; Kilicaslan, I.; Canakci, M. Numerical evaluation by models of load and spark timing effects on the in-cylinder heat transfer of a SI engine. *Numer. Heat Transf. Part A Appl.* **2009**, *56*, 444–548. [CrossRef]
33. Wang, X.; Stone, C.R. A study of combustion, instantaneous heat transfer, and emissions in a spark ignition engine during warm-up. *Proc. Inst. Mech. Eng. Part D J. Automob. Eng.* **2008**, *222*, 607–618. [CrossRef]




© 2020 by the authors. Licensee MDPI, Basel, Switzerland. This article is an open access article distributed under the terms and conditions of the Creative Commons Attribution (CC BY) license (http://creativecommons.org/licenses/by/4.0/).